Optics Communications 407 (2018) 367–374

Contents lists available at ScienceDirect

Optics Communications

journal homepage: www.elsevier.com/locate/optcom

Phase unwrapping in digital holography based on non-subsampled contourlet transform

Xiaolei Zhang [a], Xiangchao Zhang [a,*], Min Xu [a], Hao Zhang [a], Xiangqian Jiang [a,b]

[a] *Shanghai Engineering Research Center for Ultra-Precision Optical Manufacturing, Fudan University, Shanghai 200438, PR China*
[b] *EPSRC Future Metrology Hub, University of Huddersfield, Huddersfield, HD1 3DH, UK*

ARTICLE INFO

Keywords:
Interferometry
Digital holography
Phase unwrapping
Contourlet
Speckle

ABSTRACT

In the digital holographic measurement of complex surfaces, phase unwrapping is a critical step for accurate reconstruction. The phases of the complex amplitudes calculated from interferometric holograms are disturbed by speckle noise, thus reliable unwrapping results are difficult to be obtained. Most of existing unwrapping algorithms implement denoising operations first to obtain noise-free phases and then conduct phase unwrapping pixel by pixel. This approach is sensitive to spikes and prone to unreliable results in practice. In this paper, a robust unwrapping algorithm based on the non-subsampled contourlet transform (NSCT) is developed. The multiscale and directional decomposition of NSCT enhances the boundary between adjacent phase levels and henceforth the influence of local noise can be eliminated in the transform domain. The wrapped phase map is segmented into several regions corresponding to different phase levels. Finally, an unwrapped phase map is obtained by elevating the phases of a whole segment instead of individual pixels to avoid unwrapping errors caused by local spikes. This algorithm is suitable for dealing with complex and noisy wavefronts. Its universality and superiority in the digital holographic interferometry have been demonstrated by both numerical analysis and practical experiments.

1. Introduction

In optical engineering, plenty of interferometry based measurement methods have been developed, such as the phase-shifting interferometry, interferometric synthetic aperture radar [1], digital shearography [2], and incoherent optical frequency comb interferometry [3]. Among these measuring methods, digital holography [4] has attracted extensive attention due to its capability of measuring complex features. Phase unwrapping is an essential step for quantitative measurement of micro/nanocomponents because the phases obtained from interferograms are constrained between $-\pi$ and π. Unwrapped continuous phases could be obtained by adding an integral multiple of 2π to each pixel for ensuring the differences between adjacent pixels less than π. But in practice, the phases will contain errors due to the disturbances such as noise, spikes, and defects. Thus the boundary between adjacent phase levels will be mistakenly obtained. This issue is more challenging for digital holography because the complex amplitudes are obtained by the Fresnel diffraction, hence the noise and speckles are more significant in the restored wavefronts.

Existing unwrapping algorithms can be classified into path-dependent [5–9] and path-independent [10–14] methods. Path-dependent methods unwrap the phases along a continuous path specially selected. An appropriate path can be determined by identifying unpolluted measurement points or by reducing the effects of the measured noise and defects [7,9]. Some acceleration methods have also been developed to improve the computational efficiency [8]. In these methods, the choice of a proper path is not straightforward in practice, especially when the statistical distribution of noise is unknown or dependent on the specific measured objects.

Then path-independent algorithms are proposed to solve this problem. These methods filtered out the local measurement noise by minimizing an error metric properly defined. The conventional least squares approach behaves poorly in dealing with large-scale noise and spikes [13]. Hence new objective functions are applied, e.g. the L-p norm [10], the total variation regularization [11] and other smooth basis functions [12]. These methods often have good robustness, but they tend to over-smooth the phase maps and take too much time in computation.

Furthermore, some unwrapping algorithms based on the multiscale wavelet transforms are developed [15]. The multiscale decomposition

---

[*] Corresponding author.
E-mail address: zxchao@fudan.edu.cn (X. Zhang).

https://doi.org/10.1016/j.optcom.2017.09.057
Received 7 July 2017; Received in revised form 15 September 2017; Accepted 16 September 2017
0030-4018/

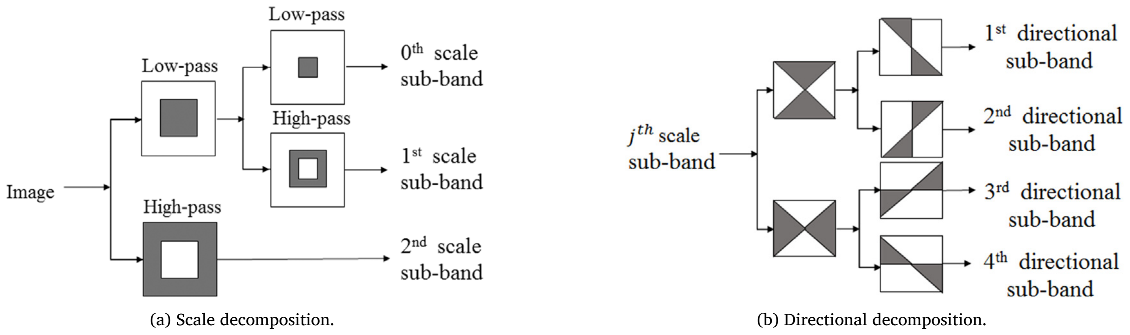

(a) Scale decomposition.

(b) Directional decomposition.

Fig. 1. Procedure of non-subsampled contourlet transform.

could enhance the boundary between adjacent phase levels and reduce the number of decomposed coefficients by subsampling. Therefore the efficiency of calculation is significantly improved. However, this approach has two main problems. First, the directional boundaries cannot be extracted accurately in the limited decomposed directions. Second, the pseudo-Gibbs effect can be caused by the subsampling in the wavelet transform [16]. As a result, distortions occur around the boundaries between different phase levels.

Current unwrapping algorithms are either inefficient or unrobust for dealing with noisy phase maps. Considering the main issue is to identify the boundaries between adjacent phase levels, the key to reliable unwrapping turns out to be the accurate segmentation of phase maps. A new unwrapping algorithm is proposed in this paper. The non-subsampled contourlet transform (NSCT) [17] is used for accurate segmentation due to its shift-invariance and sparse representation of directional features.

This paper is organized as follows. The non-subsampled contourlet transform is introduced in Section 2, and the methodology of the phase unwrapping algorithm is described in Section 3. Sections 4 and 5 present numerical and practical experiments. Finally the paper is summarized in Section 6.

2. Non-subsampled contourlet transform

Non-subsampled contourlet transform consists of two stages, namely the non-subsampled pyramid (NSP) [17] and the non-subsampled directional filter bank (NS-DFB) [18].

At the *j*th step of the NSP decomposition, the input image is decomposed first into two parts according to their scales. The small-scaled components are defined as the *j*th scale sub-band. Then the large-scaled component is further decomposed, and the (*j*-1)th scale sub-band is obtained. Implementing this NSP decomposition repetitively until the zeroth scale sub-band, i.e. the largest scale component is worked out. It is worth mentioning that the subsampling in the conventional contourlet transform is replaced by the upsampling of the corresponding low-pass filter [17]. Hence the size of each scale sub-band remains the same as that of the input image. For the sake of clarity, the scale decomposition is depicted in the Fourier transform domain in Fig. 1(a). The dark regions denote the support frequency region of each scale.

Then each scale sub-band is decomposed into different directions using the NS-DFB [18] except for the zeroth scale sub-band. NS-DFB is a tree-structured filter bank that splits the Fourier frequency plane into directional wedges. The subsampling in the conventional directional decomposition is replaced by linear transformation [18]. Consequently, the size of each directional sub-band is the same as that of the corresponding scale sub-band. Fig. 1(b) shows the NS-DFB decomposition of a scale sub-band into four directional sub-bands.

This transform possesses two remarkable advantages. The first one is its capability of multiscale and multidirectional decomposition. This could enhance salient features like contours and edges, and then noise and local defects can be separated straightforwardly. The second one is the shift-invariance guaranteed by non-subsampling. The directional features extracted in different sub-bands have the same location, therefore distortions occurring in reconstruction and unwrapping are avoided. As a well-developed technology, the detailed derivation of NSCT is omitted here. The program codes of NSCT can be found in [17].

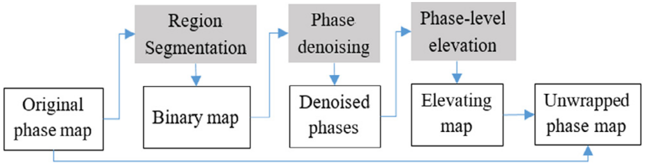

Fig. 2. Flowchart of the proposed unwrapping algorithm.

3. Multiscale and multidirectional phase unwrapping

The proposed unwrapping algorithm consists of region segmentation, phase denoising, and phase-level elevation. The main flowchart is given in Fig. 2. The wrapped phases are first transformed with NSCT. The boundaries between different phase levels are subsequently extracted, and the whole phase map is segmented into several phase regions. Then each region is denoised independently. After eliminating the phase differences between adjacent phase levels by elevation of multiple 2π, the final unwrapped phase map is obtained. The detailed procedure is described in the following subsections.

3.1. Region segmentation

The wrapped phase map is decomposed first with NSCT, and the multiscale and multidirectional subbands are obtained. The recommended numbers of decomposed scales and directions are three and four, respectively. Because most of noise and spikes remain in the small-scaled components, the second scale sub-band is ignored, and only the zeroth and first scale sub-bands are used for segmentation. In the zeroth scale sub-band, rough boundaries could be extracted straightforwardly by binarization. While the first scale sub-band has four directional sub-bands, thus the directional features corresponding to the region boundaries are enhanced. After simple thresholding with the root-median-square or multiscale thresholds [19,20], some roughly connected contours are obtained. Mathematical morphology operators OPEN and CLOSE [21,22] are used subsequently. The former connects the contour filaments and the latter eliminates the isolated defects. After fusing the directional sub-bands, an approximate boundary can be obtained. The functions used in the thresholding and morphological operations are commonly applied in image processing, hence the program is easy to implement.

The final step is to match the results of the two scales. Only the extracted features existing in both scales comprise the correct boundaries. Fig. 3 presents the main procedure of region segmentation.